

A Portable Cognitive Tool for Engagement Level and Activity Identification

T. Teo, S. W. Lye, Y. F. Li, Z. Zakaria

Abstract—Wearable devices such as Electroencephalography (EEG) hold immense potential in the monitoring and assessment of a person's task engagement. This is especially so in remote or online sites. Research into its use in measuring an individual's cognitive state while performing task activities is therefore expected to increase. Despite the growing number of EEG research into brain functioning activities of a person, key challenges remain in adopting EEG for real-time operations. These include limited portability, long preparation time, high number of channel dimensionality, intrusiveness, as well as level of accuracy in acquiring neurological data. This paper proposes an approach using a 4-6 EEG channels to determine the cognitive states of a subject when undertaking a set of passive and active monitoring tasks of a subject. Air traffic controller (ATC) dynamic-tasks are used as a proxy. The work found that using a developed channel reduction and identifier algorithm, good trend adherence of 89.1% can be obtained between a commercially available brain computer interface (BCI) 14 channel Emotiv EPOC+ EEG headset and that of a carefully selected set of reduced 4-6 channels. The approach can also identify different levels of engagement activities ranging from general monitoring, ad hoc and repeated active monitoring activities involving information search, extraction, and memory activities.

Keywords—Neurophysiology, monitoring, EEG, outliers, electroencephalography.

I. INTRODUCTION

RECENT years have seen the increased adoption of online and remote modes for work and learning as a result of the COVID-19 pandemic [1]. In cases like these where physical attendance is not possible, effective collaborative and training methods have to be developed [2]. One key challenge is to evaluate both the state of mind and task activity engagement of the person involved. This holds true for a person who may be physically present while his state of mind may not. Currently, there is a lack of portable tools that could provide a real-time measure of the cognitive state of a person when engaging in online or remote tasks. This has subsequently led to research work being conducted to develop portable measuring devices, such as electroencephalography (EEG), to monitor the physiological level of activity in the subjects concerned [3]. A study by Yuvaraj et al. [4] found that neurophysiological response data obtained through the use of pEEG were able to provide some level of indication about one's cognitive states, as well as demonstrate functional relations to task specificity. Other research works have also seen an increased adoption of pEEG devices in clinical research (e.g., [5], [6]), driver drowsiness detection (e.g., [7]-[10]), as well as airline pilot and air traffic control officer (ATCO) workload measurements

(e.g., [11]-[14]). In this regard, the captured data could be used in a variety of real-time support mechanisms, such as dashboards and academic advising [15], [16], or in potential activity evaluation and workload and performance assessment applications which are presently under much research.

In many studies, Power Spectral Density (PSD) has been successfully employed as a parametric measure to assess cognitive responses across a wide range of mental activities – including attention (e.g., [26], [27]) – where it has been reported that different brain activities were still distinguishable even when multiple classifiers were employed [28]. PSD is a frequency domain assessment of the power distribution of EEG input signals over a given frequency range within a defined epoch [29].

Despite its merits, key drawbacks commonly faced when used in a mobile environment include (a) “noise” from redundancies stemming from its high dimensionality, which also imposes increased computational burden [17]-[19], (b) the maintenance of acceptable levels of signal-to-noise ratio over the experiment's duration [20], [21], (c) ascertaining the sensitivity and accuracy of the response to the underlying neurological processes, the performance, and specificity of the tasks [18], [22], (d) artifacts arising from the ambulatory working environment of ATCOs (e.g., muscular movement), as well as (e) long setup time required. These traits present challenges to its desirability. To address them, channel dimensionality reduction techniques involving the use of filtering, wrappers, and embedment techniques [17], [18] – have been developed to extract and identify “diffused” features brought about by sets of irrelevant or redundant information, which also sought to reduce computational burden [17]-[19], [23]-[25]. Nevertheless, a portable tool with significantly reduced channels, yet relatable to the human operator's cognitive state while undertaking online or remote activities, is still in its infancy.

This study aims to propose a portable reconfigurable BCI approach based on only 4-6 selected channels to determine the cognitive states relating to passive and active monitoring states involving memory, and information search-and-extract activities when undertaking a functional monitoring task of a subject. The work necessitates the following:

1. The establishment of a channel reduction method that could identify a small set of targeted channels capable of exhibiting similar underlying trends when compared to a full channel setup,
2. Result comparisons of the various cognitive state measures

(NTU), Singapore (e-mail: zain0004@ntu.edu.sg).

T. Teo, S. W. Lye, Y. F. Li, and Z. Zakaria are with the School of Mechanical and Aerospace Engineering, Nanyang Technological University

to activity engagement level between the proposed reduced channel method with the 14 channels of a commercially available Emotiv EPOC+ EEG headset, commonly used to capture cortical signals [30], and

3. Result validation of the proposed method used to identify the various activities when performing a functional monitoring task.

II. EXPERIMENTAL SETUP AND DESIGN

A. Experimental Setup

Dynamic air-traffic scenarios were simulated on an NLR Air Traffic Control Research Simulator (NARSIM) [31]. A radar screen displays aircraft information in one sector of an en-route airspace (see Fig. 1). Aircraft positions were updated by radar sweeps in intervals of 9.8 seconds which corresponds to one radar revolution.

In this experiment, a key functional task involving traffic monitoring is studied where a subject would be required to perform general traffic monitoring surveillance, single and repeated search-and-extract, as well as memory activities for flight information. EEG data were recorded with an Emotiv EPOC+ headset through 14 active probes, sampled at 128Hz using the linked ear reference method (Note: sampling frequency satisfies the Nyquist frequency to avoid aliasing [32]-[34]). Neural electrical activities were recorded at positions AF3, F7, F3, FC5, T7, P7, O1, O2, P8, T8, FC6, F4, F8 and AF4 through saline-soaked sensors, in a constellation defined

by the international 10-20 system (see Fig. 2) [34]. Data are then transmitted wirelessly via Bluetooth to the recording device, eliminating cumbersome wires and supporting full free movement – a condition much favored by ATCOs. The EEG data are then segmented into “epochs” based on the same time interval over 9.8 seconds for analysis.

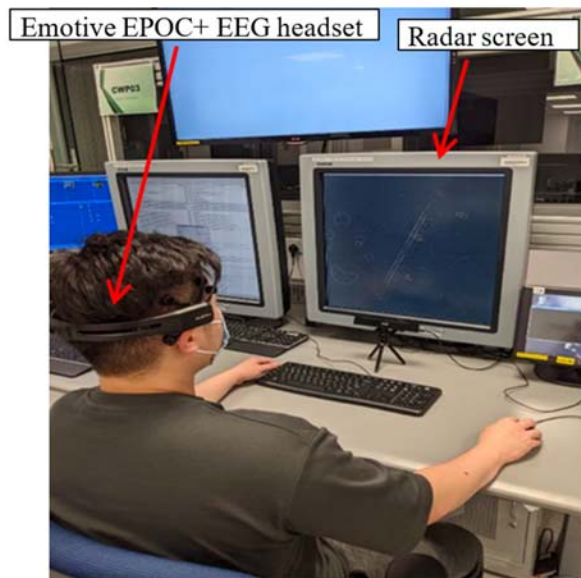


Fig. 1 NARSIM air traffic radar Controller Work Position

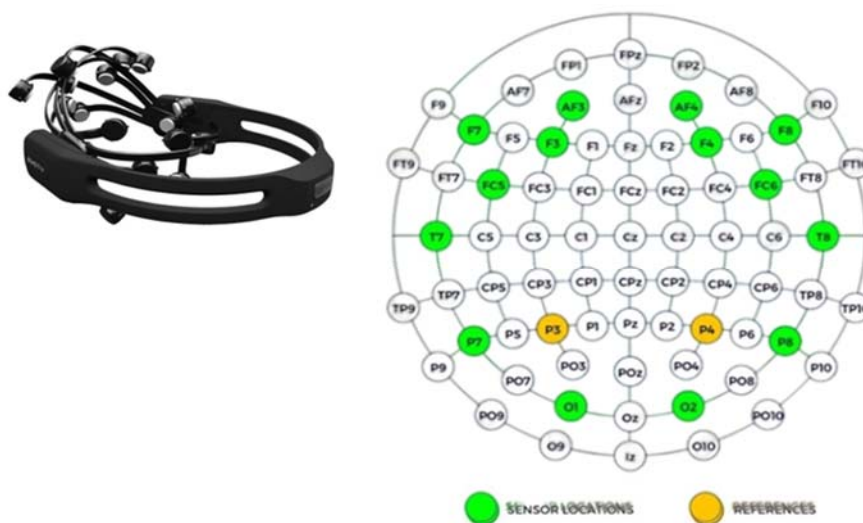


Fig. 2 Emotiv EPOC+ 14 channels headset (L) and sensor locations (R)

B. Experimental Design

The experiments involved 21 undergraduate participants (Mean age (years) = 29, SD = 5.34). Each participant would need to perform three sets of sub engagement tasks at prescribed timing throughout the 60-minute duration (see Table I). These three sub-tasks were as follows: (a) general monitoring with no query (pre-Query), (b) memory query of target flight information at the beginning and end of experimental periods

(Q1 and Q1a), and (c) single and multiple queries on search-and-extract target flights and information (Q2 and Q2a). PSD datasets were collected and then analyzed. The sample was then separated into two parts with 5 randomly selected to be used as the validation set and the remaining 16 used for as the testing set. A power analysis conducted based on the sample size of 16, with an 80% statistical power and $\alpha = 0.05$ in binary class differentiation, achieved an effect size in excess of 0.8 [35].

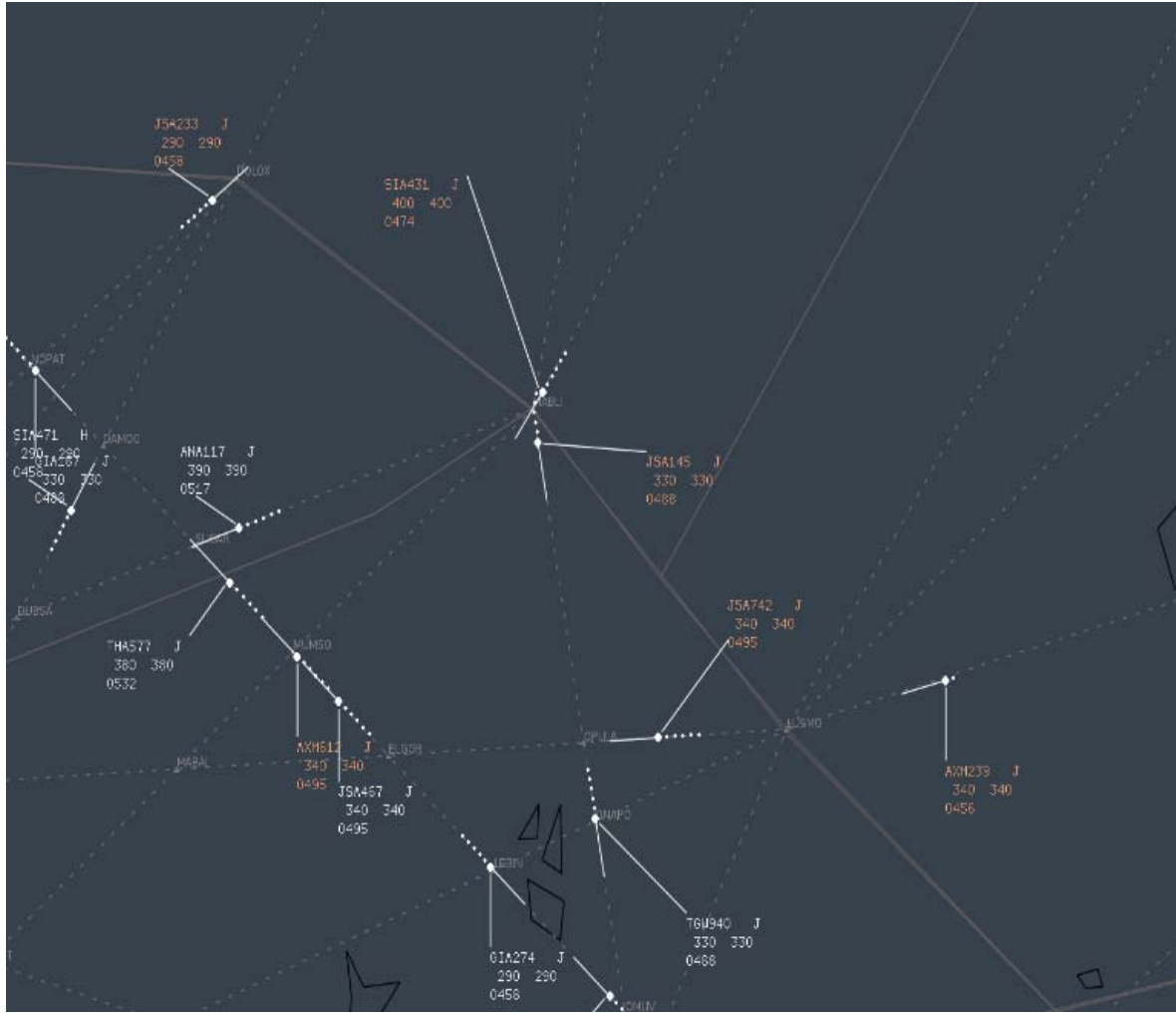


Fig. 3 Screen capture sample of the simulation screen

TABLE I
 OUTLINE OF ACTIVITIES INVESTIGATED

Time from start (min)	Query type
03:00	Pre-Query (Q1)
04:00	Memory query (Q1)
19:00	Pre-Query (Q2)
20:00	Search and extract (Q2) (single)
43:00	Pre-Query (Q2a)
44:00	Search and extract (Q2a) (multiple)
57:00	Pre-Query (Q1a)
58:00	Memory query (Q1a)

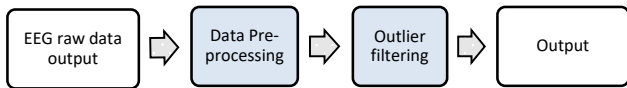


Fig. 4 A 2-step Outlier Filtering Mechanism

Participants were given 30 minutes briefing session prior to the experiments which consisted of training on the interpretation of the displayed radar traffic information, as well as the tasks to be performed. Approval from the University's Institutional Review Board has been obtained.

III. DEVELOPMENT OF AN OUTLIER FILTERING MECHANISM

Fig. 4 shows a 2-step flow of the outlier filtering mechanism used to derive at a processed set of EEG data from the raw form for the next steps of channel identification and reduction.

A. EEG Data Pre-Processing

For this study, raw EEG data were first processed offline in the software program MATLAB. The EEG data stream was then synchronized with the NARSIM radar frames by applying time stamps and then subjected to a zero-phase, 4th order Butterworth filter with high- and low-pass cut-off frequencies set at 1 Hz and 49 Hz respectively. Low-pass cut-off at 49 Hz will exclude powerline interference (50 Hz), and high-pass at 1 Hz will remove interference from DC components and bioelectric flowing potentials (breathing, etc.) [36], [37]. Gross eyeblink artifacts were removed by performing Independent Component Analysis (ICA) through the MATLAB extension EEGLab [42]. To determine an epoch frame, this is done over a frequency range of 1 Hz-49 Hz through a non-parametric Welch's method (MATLAB function 'pwelch'). An NFFT of 1024 and resolution of 0.125 Hz over a 256 Hanning window length was used. This was followed by obtaining the

Power Spectral Densities (PSD) of an epoch over 9.8s. This is to synchronize the frame timing of the EEG raw data with radar data. In this work, one EEG epoch consists of 1254 frames (9.8 sec/128 Hz) and is matched to the radar frame duration of 9.8s. To determine the PSD value for one 9.8s frame, all the PSD values within an epoch were summed and divided by 1254 (the number of frames). Any slippage in recording due to instrument latency is rendered insignificant in respect of the 9.8s epochs.

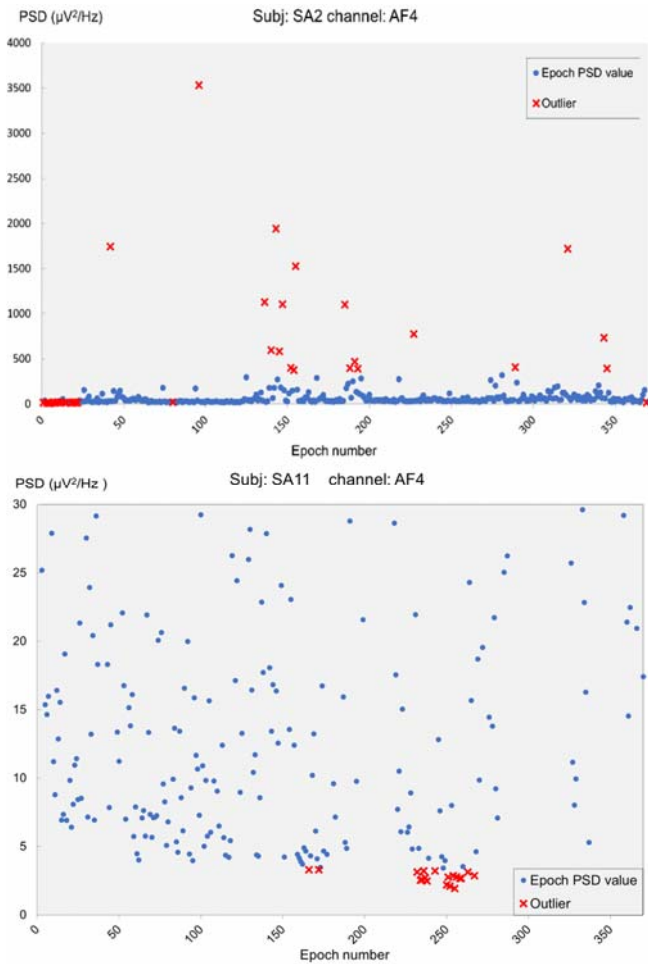


Fig. 5 Typical EEG output with discrete outliers scattered across the experiment duration; the outlier points are highlighted in red crosses amidst the stable data in blue to illustrate their distribution across the experiment duration

Fig. 5 shows a typical data output plot of a channel for a given participant. From the figure, one can observe that there exists a small number of single momentary and discrete global data outliers caused by artifacts or momentary loss of contacts. To determine the underlying state of an activity, these outliers would need to be filtered off as such global outliers or signal distortions could greatly influence the validity and stability of the recorded signals. This finding is consistent with the results from other researchers [38], [49].

B. Outlier Filtering

It was observed that most of the recorded EEG data values

exhibited a non-normal distribution profile with a high degree of right-skew, which would compromise the analyses when based only on Gaussian features [40]. Further observations also revealed that the skewness was attributable to non-neurophysiological artifacts introduced in the data acquisition phase, which effectively causes a negative effect on the signal-to-noise ratio, as reported by [24], [33], and [41].

Owing to the variety in the distribution of the values (e.g., bimodality, high degree of right/left skewness, etc.), a filter mechanism would need to be established to remove these global outliers. The approach proposed by this paper is to establish percentile limits to remove these global outliers which occur at the extreme ends of the data set while maintaining a sizeable and stable set of PSD values that can provide a good measure of the actual underlying state of an activity.

Table II shows the relationship between the set of boundary limits based on percentiles and the mean and median values of the data set as presented in Fig. 5. In this study, both the median and mean values are considered because any increase in brain activity would jointly affect both MEDIAN as well as MEAN. The appearance of any number of artifacts other than that induced by the true sustained cognitive behavior will therefore skew the MEAN away from the MEDIAN. Conversely at the other end, the dropping of signals due to poor or intermittent scalp contact would also reduce the MEDIAN together with the MEAN to a depressively low number as compared to the global set of results, which can then be flagged or sieved out.

Using channel T7 (located above the left ear) as an illustration, Table II shows the step changes of the mean values with variation in the percentile limits imposed. From the 5th-95th percentile range onwards, the changes in the mean and median values have stabilized (to within 5%) and do not change as significantly as they have done in the previous percentile ranges. Thus, in this work, the boundary filter limits for outliers were set at the 5th and 95th percentiles for all channels (here on referred to as P5-95). This percentile setting was then performed on channels O2 (back of head) and F4 (right forward), with similar findings observed (see Fig. 6). With this percentile filtering range set and applied, the data set is now presented in Figs.7 (a) and (b) with the outliers highlighted in red.

IV. ESTABLISHMENT OF A CHANNEL REDUCTION METHODOLOGY

Counting reduced computational load among many other advantages, the objective for channel selection and reduction is to select a desired set of reduced channels (from any number of original N-channels) that displays similar characteristics and trend responses to the original setup used in the capture of neural responses to the stimuli for a group of subjects. And for the fact that each participant exhibits a different cognitive level and thereby PSD values, the aim is therefore to identify channels (from the set of filtered data) where the recorded PSD values are representative of the group of test subjects to within a prescribed confidence level, set at 95% in this work.

A. Criteria for the Selection of Channels

Fig. 8 shows the 95% confidence level range of mean and median values exhibited in each of the 14 channels after the outliers were removed. By representing the values on a compact logarithmic (base 10) scale, an underlying trend pattern can clearly be observed - where localized activation of the various neural regions during the tasks has resulted in differing PSD boundary limits over each of the 14 channels [42]. From this, Fig. 9 is produced which shows the 14-channel PSD plots for channels that are deemed acceptable in the test group of 16 subjects. Colored boxes indicate the channels that contained filtered PSD values outside the 95% confidence level (amongst the group of 16). As an illustration, the row boxes for SA2 do not contain any colored boxes. This indicates that the set of PSD values for the subject are all within the 95% confidence level among the group of test subjects in all the channels. For SA1 subject, 10 of the channels (F7, F3, FC5, P7, O1, T8, FC6, F8 and AF4) contained data values that are outside the group confidence level.

TABLE II
MEAN AND MEDIAN VALUE CHANGES ACROSS PERCENTILE LIMITS ON CHANNEL T7 (N=16)

Percentile Limits	Mean PSD	Step change	Median PSD	Step change
0-100	183.254	-	56.224	-
1-99	138.680	24.3%	56.222	0.003%
2-98	115.251	16.9%	56.211	0.021%
3-97	106.758	7.4%	56.211	0.000%
4-96	98.858	7.4%	56.210	0.000%
5-95	93.477	5.4%	56.210	0.000%
6-94	90.174	3.5%	56.209	0.002%
7-93	86.291	4.3%	56.209	0.000%
8-92	82.606	4.3%	56.083	0.225%
9-91	80.428	2.6%	56.083	0.000%
10-90	77.967	3.1%	56.083	0.000%

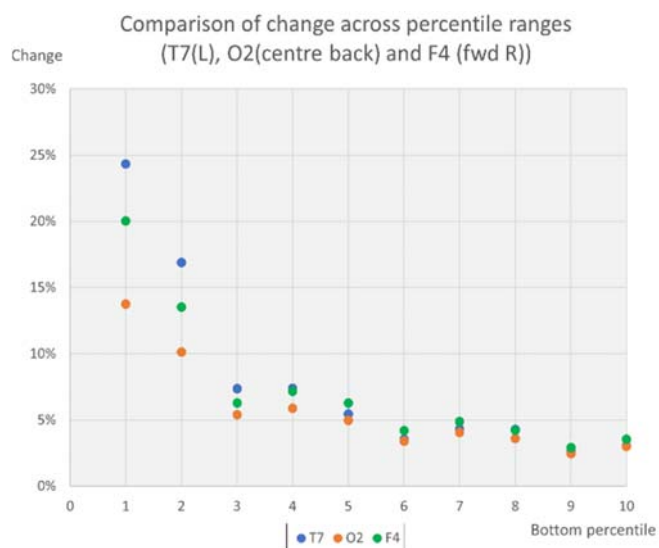


Fig. 6 Step change (%) in mean values with the variation in percentile limits imposed; the x-axis shows the bottom percentile figure of the limits, e.g., where x = 3, the 3rd-97th percentile limits is represented, and x = 5 likewise represents the 5th-95th percentile limits

Through inspection of the columns, eight channels of {FC5, T7, P7, O1, O2, F4, F8 and AF4} were found to be the most stable and consistent amongst the group with most of the PSD values falling within the 95% confidence level.

For the 4-channel reduction, {T7, P7, O2 and AF4} are selected as they not only provide an evenly distributed spatial representation across the scalp topography, but also take into consideration the neural characteristics of the associated cortical areas represented by the respective channels that match the task demands. This stems from evidence from Positron Emission Tomography (PET) scans and Event-Related Potentials (ERP) studies where episodic retrieval tasks (involving recall and recognition) have shown to have elicited a dominance of neural activities in the right frontal (e.g., F4, F8) and prefrontal areas (e.g., AF4) [43]. Additionally, Magen et al. [44] found evidence of cortical activation in the Posterior Parietal Complex (PPC) in tasks where short-term memory load were imposed, while attentional demands were reflected in the parietal region of the brain (i.e., closest probes P7 or P8) in Rushworth et al. [45] and Behrmann et al.'s [46] research.

Whilst Norbre et al. [47] had confirmed the importance of the parietal cortex in visual search, Kojima & Suzuki [48] had also surmised a possible correlation between attention and activation of the occipital lobes (channels O1 and O2) though increased blood flow observed using Near Infrared Spectroscopy (NIRS). These evidences corroborate with findings that attention-related neural activities being closely associated with the parietal, temporal, and prefrontal cortices of the brain (corresponding to probe regions Tx, Px and AFx) [49]-[51]. Subsequently for the 6-channel reduction, {O1 and F4} could be included in the above selection set to enhance data reliability.

B. Assessment of Selection Success

During the course of this study, an increase in the EEG channels' PSD readings were generally observed when queries were applied. This involved measuring the total PSD of each channel: (a) before the task ("Pre-query"), and (b) while the participants were carrying out the required tasks (e.g., search-and-extract target information) ("Query"). "Pre-query" has been taken as *one* minute (6 epochs) before the start of query, while the Query period was defined as the time period when query was applied, with the inclusion of a further one minute from the end of query (with an overlap of one epoch), to improve the signal-to-noise ratio from the averaging operation and cater for any latency between stimuli and the formation of stable waveform responses [34], [39].

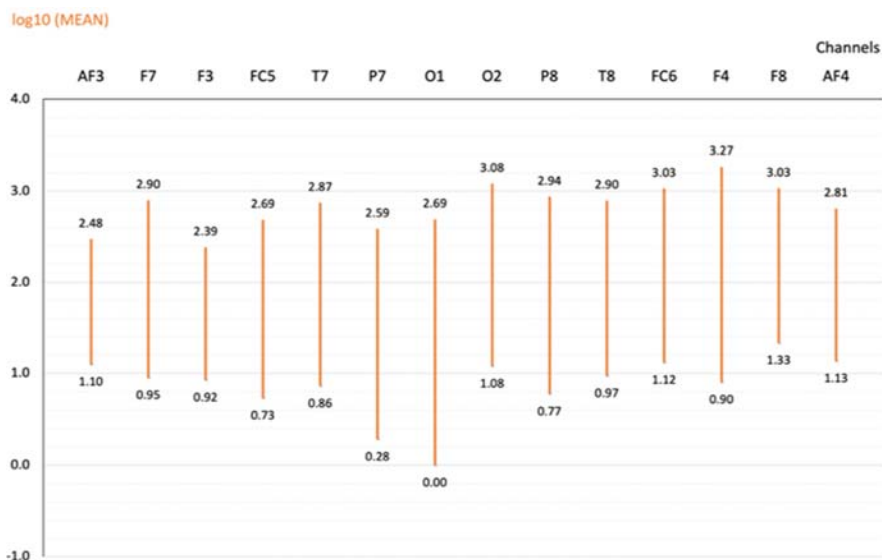
To arrive at the Query and Pre-Query PSDs, representative "Epoch PSDs" were first obtained by taking the arithmetic average of all 14 channels that belongs to that subject *at each epoch*, represented by the following operation:

$$\text{Epoch PSD} = \frac{1}{14} \sum_{i=1}^{14} (\text{PSD})_{\text{channel } i} \quad (1)$$

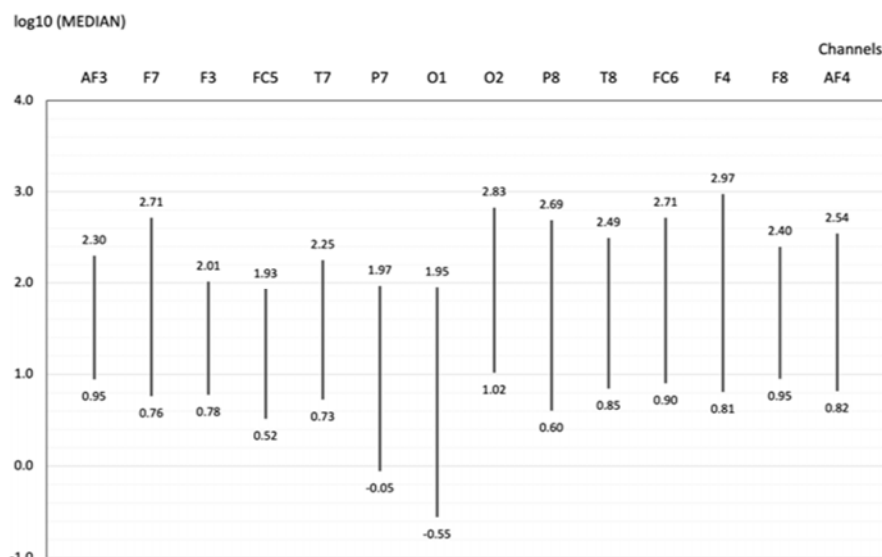
$P_{5.95}$ was then applied to the group of epochs under the Pre-Query and Query periods respectively to trim the outliers, before calculating the trimmed mean for the periods. The output would be a Pre-Query PSD and a Query PSD for the subject in

question for that specific task-query. The process is repeated for all other queries in all subjects. At this juncture, one needs to

note that this method for PSD formulation is not without its limitations.



(a)



(b)

Fig. 7 Mean and Median ranges of values for all channels after the outlier filtering mechanism was applied (displayed in logarithmic scales for compactness)

While studies have shown that the various EEG frequency oscillations (delta (1-3 Hz), theta (3-7 Hz), alpha (8-12 Hz), beta (12-29 Hz), and gamma (30-40 Hz)) may exhibit non-homogenous activation behavior under different stimuli, one notes that Liu et al [33] and Peng et al. [34] have both managed to achieve greater degree of accuracy in detecting attentiveness by incorporating more features, with the former using the PSDs of the alpha, beta, delta and theta frequency bands, and concluding that each feature exerts a positive influence on classification accuracy. On the contrary, we propose a "Gestaltist" approach instead – by using PSD of the total

frequency spectrum as a feature, where changes in frequency components were analyzed in totality, instead of evaluating through the individual frequency bands. The basis for this rests on the numerous observations made during in-house trial experiments where the total PSD during Query was found to be generally higher in magnitude than the Pre-Query PSDs.

Additionally, research also suggested that the brain's allocation of cortical resources could vary by intelligence and expertise [52], task difficulty and familiarity [53], [54] through the phenomenon of *neural efficiency*. This gives rise to the observed variations in PSD output ranges as well as

performance results. This, too, was not moderated in this study.

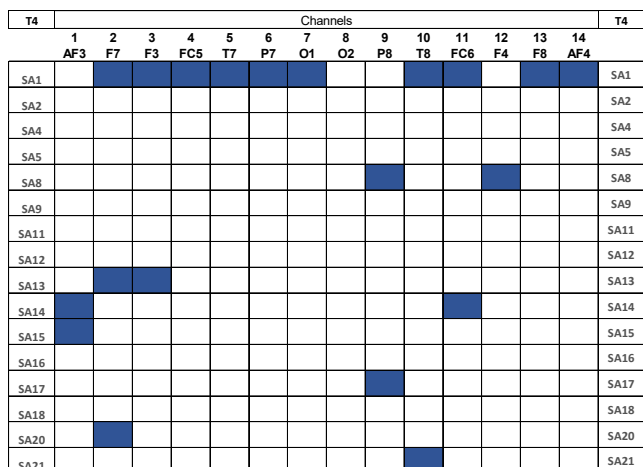


Fig. 8 The montage of value extreme channels at 95% C.I.; Shaded boxes represent channels that exhibit values that are extreme in respect of the global range

	14ch	6ch	4ch
SA1	+	+	+
SA2	+	+	+
SA4	E	E	+
SA5	+	+	+
SA8	E	E	E
SA9	+	+	+
SA11	+	+	+
SA12	N	N	N
SA13	+	+	+
SA14	+	+	+
SA15	+	+	+
SA16	+	+	+
SA17	+	+	+
SA18	N	N	N
SA20	N	N	N
SA21	+	+	+

Fig. 9 Response matching through reduction from 14-channels to 6- and 4-channels on task-query Q2

Notwithstanding the above, this feature was used in the following channel selection and reduction methodology, and subsequently to gauge the fitness of the selected channel configuration in capturing the response characteristics of the full channel set. This method however is independent of the number and type stimuli as well as the number of EEG channels utilized. The resultant channels selected are therefore "customized" to the designed tasks.

V. RESULT AND DISCUSSION

A. Comparative Measure of Activity between the Proposed Reduced Channels Approach and the Standard 14 Channels

1. Classification of Brain Activity Measure

Having observed the wide range of PSD values individuals were capable of exhibiting (e.g., 2500 $\mu\text{V}^2/\text{Hz}$ vs 250 $\mu\text{V}^2/\text{Hz}$),

which could be due to unmoderated neural efficiency factors, the metric used for comparative evaluation in this study would be based on percentage change of magnitude in response to the stimuli rather than the raw PSD values. This is for the following reasons:

- Collective analysis of the testing group data based on raw values may not be representative owing to wide variances between test subjects. The EEG data for each subject have to be examined individually.
- Interference from uncontrolled factors such as unmoderated emotional states could have contributed to the observed background rise in brainpower as the experiment progresses. Therefore, any analysis will need to tap into second level characteristics of trends and change-proportions in order to extract the hidden patterns of behavior.

Following this, responses upon a stimulus being applied are classified into 3 main types namely:

- A positive response where the relative PSD magnitude change is positive (+),
- A negative response where the relative PSD magnitude change is negative (N), and
- A neutral response where the relative PSD magnitude change are within a threshold margin and are thus deemed unchanged (E). This is in recognition of the possibility that the combined PSD of the various neural oscillations at the Query stage yielding a similar value as the Pre-Query PSDs, even though the individual oscillations have undergone antagonistic changes in magnitude separately. To this, a study was performed separately to determine the best compromise between error coverage and a stable response-matching accuracy. This value was determined to be 5%, and is subsequently adopted in the investigation.

2. Assessing the Success of the Reduction Method: Response-Matching

The success of the reduction method (4 or 6 channel) will be gauged by how well the participants' responses can be compared with the original set of 14 channels over 4 set of task queries. The evaluation analysis will be made based on the formulated training set of 16 participants and subsequently on a validation test set composed of 5 new participants. To illustrate, Fig. 9 shows the responses of the training set between 14-, 6- and 4-channels across task-query Q2. Of the 16 participants, for the 14-channel configuration (column 1), eleven responses were positive (+), three responses were negative (N), whilst two responses were neutral (E).

In the 6-channel reduction (column 2), it can be observed that its responses are similar to that of the 14 channels across each of the participants. This means that for SA1, both the 14 and 6 channel configurations registered a "+" response. There is therefore a 100% response matching between both channel configurations across all participants.

In the 4-channel reduction (column 3), the mapping was almost 100% except for participant SA4 where a neutral (E) was mapped to a positive (+). This gives a mapping accuracy of 15 out of 16 (93.8%).

Table III shows the response mapping for the four task-queries between the three channel configurations (14, 6 and 4). It can be seen that the 14-to-6 reduction produced a response-matching range from 75.0% to 100% whilst in the 14-to-4 reduction is between 81.3% to 93.8%. For the 14-to-6 reduction, when broken down into the task-query types, Memory tasks (Q1 and Q1a) yielded an average 84.4% accuracy whilst Search-and-Extract tasks (Q2 and Q2a) yielded 93.8%. For the 14-to-4 reduction, Memory tasks produced an average of 90.7% matching while that for Search-and-Extract tasks was 87.6%. On the average, an 89.1% average matching accuracy was obtained in both channel reduction configurations. At the surface level, this success of the methodology is evident.

In terms of change magnitudes, 2-tailed paired sample *t*-tests were performed between the 14-channels and the reduced 6-channels for the 4 task-queries. No statistical significance was observed at $\alpha = 0.05$ (Q1: $t(15) = 1.359, p = 0.194$; Q2: $t(15) = 0.620, p = 0.544$; Q2a: $t(15) = 0.988, p = 0.339$; Q1a: $t(15) = 0.017, p = 0.987$). This was similarly the case for the reduced 4-channels (Q1: $t(15) = -0.461, p = 0.652$; Q2: $t(15) = 1.021, p = 0.324$; Q2a: $t(15) = 0.608, p = 0.552$; Q1a: $t(15) = -0.239, p = 0.815$).

The above results indicate that no significant magnitude change between the 14-channel configuration to that of the proposed channel reduction configurations.

TABLE III
RESPONSE MATCHING FOR 14-TO-6 AND 14-TO-4 CHANNELS REDUCTION
ACROSS 4 TASK QUERIES

	Channel Reduction	Q1 (%)	Q2 (%)	Q2a (%)	Q1a (%)
Training	14 to 6	75.0	100.0	87.5	93.8
	14 to 4	87.5	93.8	81.3	93.8
Validation	14 to 6	100.0	80.0	100.0	100.0
	14 to 4	100.0	80.0	100.0	100.0

B. Validation of Results on the Identification of Activity Engagement of the Proposed System

For the purposes of validation, a set consisting of 5 randomly chosen participants were extracted from the collected data but excluded from the training set. Applying similar methodical steps of outlier-removal and the same channel-reduction configuration, the response results are also listed in Table III for easy comparison.

It can be seen that the result was uniform across the 6-channel and 4-channel reductions. Except for task-query Q2 being 80.0%, the matching responses was 100% for task-queries Q1, Q2a and Q1a. This produced an average of 95.0% matching accuracy for both reduction configurations. In the case of validation, memory tasks yielded an average matching accuracy of 100% whilst a 90.0% average accuracy was obtained in Search-and-Extract tasks.

In terms of change magnitudes, 2-tailed paired sample *t*-tests performed between the 14-channels and 6-channels and 4-channels similarly yielded no statistical significance at $\alpha = 0.05$ (6-channel: Q1: $t(4) = 0.408, p = 0.704$; Q2: $t(4) = -1.013, p = 0.368$; Q2a: $t(4) = -1.544, p = 0.197$; Q1a: $t(4) = 2.223, p = 0.09$,

4-channel: Q1: $t(4) = 0.390, p = 0.716$; Q2: $t(4) = -1.007, p = 0.371$; Q2a: $t(4) = -0.951, p = 0.395$; Q1a: $t(4) = 2.610, p = 0.059$).

VI. CONCLUSION

In this study, a methodology for EEG channel reduction was proposed. Results showed that the method was able to yield a good level of response matching relating to Memory and Search-and-Extract task-queries across the participants.

The above finding was supplemented by the proposed outlier filtering method developed using the curtailed 5th to 95th percentile of the range, P_{5-95} . This led to a method for defining valid working ranges across the experiments. A resultant map of good channels can then be produced which one can utilize as a guide in analysis for channel selection and reduction.

In addition, it points to a need for personalizing the devices for real-world application due to the large variances between individuals. Also observed is the need to have participants prepared for the oncoming tasks before applying the task-queries, as the background readings could be affected by uncontrolled factors that may have neural significance.

VII. LIMITATIONS

As the placement and setup of EEG electrodes were administered by non-trained professionals, the accuracy and validity of the recorded data could pose an issue to its analysis, which were evident during the course of the study. Also, with the sample size as limitation, the study's assumptions of the selected features tending towards Gaussian in the first part would need further investigation. The finding would be more robust with the involvement of more participants.

ACKNOWLEDGMENTS

This research is supported by the Civil Aviation Authority of Singapore, Workforce Development Applied Research Fund, and Nanyang Technological University, Singapore under their collaboration with the Air Traffic Management Research Institute. Any opinions, findings and conclusions or recommendations expressed in this material are those of the authors and do not reflect the views of the Civil Aviation Authority of Singapore nor the organizations mentioned.

REFERENCES

- [1] J. Bryson and L. Andres, "Covid-19 and rapid adoption and improvisation of online teaching: curating resources for extensive versus intensive online learning experiences", *Journal of Geography in Higher Education*, vol. 44, no. 4, pp. 608-623, 2020. Available: 10.1080/03098265.2020.1807478.
- [2] W. Bao, "COVID -19 and online teaching in higher education: A case study of Peking University", *Human Behavior and Emerging Technologies*, vol. 2, no. 2, pp. 113-115, 2020. Available: 10.1002/hbe2.191.
- [3] P. Kumari, L. Mathew, and P. Syal, "Increasing trend of wearables and multimodal interface for Human Activity Monitoring: A Review," *Biosensors and Bioelectronics*, vol. 90, pp. 298-307, 2017.
- [4] R. Yuvaraj, S. W. Lye, and H. J. Wee, "A real time neurophysiological framework for general monitoring awareness of air traffic controllers," *2020 IEEE Asia-Pacific Conference on Computer Science and Data Engineering (CSDE)*, 2020.
- [5] H. Kiiski, M. Bennett, L. M. Rueda-Delgado, F. R. Farina, R. Knight, R.

- Boyle, D. Roddy, K. Grogan, J. Bramham, C. Kelly, and R. Whelan, "EEG spectral power, but not theta/beta ratio, is a neuromarker for adult ADHD," *European Journal of Neuroscience*, vol. 51, no. 10, pp. 2095–2109, 2020.
- [6] S. Puma, N. Matton, P.-V. Paubel, É. Raufaste, and R. El-Yagoubi, "Using Theta and Alpha Band Power to assess cognitive workload in multitasking environments," *International Journal of Psychophysiology*, vol. 123, pp. 111–120, 2018.
- [7] J. LaRocco, M. D. Le, and D.-G. Paeng, "A systemic review of available low-cost EEG headsets used for drowsiness detection," *Frontiers in Neuroinformatics*, vol. 14, 2020.
- [8] W. Li, Q.-chang He, X.-min Fan, and Z.-min Fei, "Evaluation of driver fatigue on two channels of EEG Data," *Neuroscience Letters*, vol. 506, no. 2, pp. 235–239, 2012.
- [9] G. Li, B.-L. Lee, and W.-Y. Chung, "Smartwatch-based wearable EEG system for driver drowsiness detection," *IEEE Sensors Journal*, vol. 15, no. 12, pp. 7169–7180, 2015.
- [10] S. Majumder, B. Guragain, C. Wang, and N. Wilson, "On-board drowsiness detection using EEG: Current status and future prospects," *2019 IEEE International Conference on Electro Information Technology (EIT)*, 2019.
- [11] P. Aricò et al., "Adaptive Automation Triggered by EEG-Based Mental Workload Index: A Passive Brain-Computer Interface Application in Realistic Air Traffic Control Environment", *Frontiers in Human Neuroscience*, vol. 10, 2016. Available: 10.3389/fnhum.2016.00539.
- [12] G. Borghini et al., "EEG-Based Cognitive Control Behaviour Assessment: an Ecological study with Professional Air Traffic Controllers", *Scientific Reports*, vol. 7, no. 1, pp. 1-16, 2017. Available: 10.1038/s41598-017-00633-7.
- [13] D. Dasari, G. Shou and L. Ding, "ICA-Derived EEG Correlates to Mental Fatigue, Effort, and Workload in a Realistically Simulated Air Traffic Control Task", *Frontiers in Neuroscience*, vol. 11, 2017. Available: 10.3389/fnins.2017.00297.
- [14] F. Dehais et al., "Monitoring Pilot's Mental Workload Using ERPs and Spectral Power with a Six-Dry-Electrode EEG System in Real Flight Conditions", *Sensors*, vol. 19, no. 6, p. 1324, 2019. Available: 10.3390/s19061324.
- [15] W. Matcha, N. A. Uzir, D. Gasevic, and A. Pardo, "A systematic review of empirical studies on learning analytics dashboards: A self-regulated learning perspective," *IEEE Transactions on Learning Technologies*, vol. 13, no. 2, pp. 226–245, 2019.
- [16] A. Pardo, F. Han, and R. A. Ellis, "Combining University student self-regulated learning indicators and engagement with online learning events to predict academic performance," *IEEE Transactions on Learning Technologies*, vol. 10, no. 1, pp. 82–92, 2017.
- [17] T. Alotaiby, F. El-Samie, S. Alshebeili and I. Ahmad, "A review of channel selection algorithms for EEG signal processing", *EURASIP Journal on Advances in Signal Processing*, vol. 2015, no. 1, 2015. Available: 10.1186/s13634-015-0251-9.
- [18] M. Z. Baig, N. Aslam, and H. P. Shum, "Filtering techniques for channel selection in motor imagery EEG applications: A survey," *Artificial Intelligence Review*, vol. 53, no. 2, pp. 1207–1232, 2019.
- [19] J. Zhang, M. Chen, S. Zhao, S. Hu, Z. Shi, and Y. Cao, "Relief-based EEG sensor selection methods for emotion recognition," *Sensors*, vol. 16, no. 10, p. 1558, 2016.
- [20] A. Gevins et al., "Towards measurement of brain function in operational environments", *Biological Psychology*, vol. 40, no. 1-2, pp. 169-186, 1995. Available: 10.1016/0301-0511(95)05105-8.
- [21] S. Saha, K. A. Mamun, K. Ahmed, R. Mostafa, G. R. Naik, S. Darvishi, A. H. Khandoker, and M. Baumert, "Progress in brain computer interface: Challenges and opportunities," *Frontiers in Systems Neuroscience*, vol. 15, 2021.
- [22] P. Arico et al., "Reliability over time of EEG-based mental workload evaluation during Air Traffic Management (ATM) tasks", *2015 37th Annual International Conference of the IEEE Engineering in Medicine and Biology Society (EMBC)*, pp. 7242 - 7245, 2015. Available: 10.1109/embc.2015.7320063.
- [23] M. Bannasar, Y. Hicks and R. Setchi, "Feature selection using Joint Mutual Information Maximisation", *Expert Systems with Applications*, vol. 42, no. 22, pp. 8520-8532, 2015. Available: 10.1016/j.eswa.2015.07.007.
- [24] L. Fang et al., "Feature selection method based on mutual information and class separability for dimension reduction in multidimensional time series for clinical data", *Biomedical Signal Processing and Control*, vol. 21, pp. 82-89, 2015. Available: 10.1016/j.bspc.2015.05.011.
- [25] I. Guyon and A. Elisseeff, "An introduction to variable and feature selection," *Journal of Machine Learning Research*, vol. 3, no. 3, pp. 1157–1182, 2003.
- [26] J. Foy and M. Foy, "Dynamic Changes in EEG Power Spectral Densities During NIH-Toolbox Flanker, Dimensional Change Card Sort Test and Episodic Memory Tests in Young Adults", *Frontiers in Human Neuroscience*, vol. 14, 2020. Available: 10.3389/fnhum.2020.00158.
- [27] A. Gupta et al., "On the Utility of Power Spectral Techniques with Feature Selection Techniques for Effective Mental Task Classification in Noninvasive BCI", *IEEE Transactions on Systems, Man, and Cybernetics: Systems*, vol. 51, no. 5, pp. 3080-3092, 2021. Available: 10.1109/tsmc.2019.2917599.
- [28] D. Bansal and R. Mahajan, EEG-based brain-computer interfaces. *Elsevier*, 2019, pp. 21-71.
- [29] R. Alam, H. Zhao, A. Goodwin, O. Kavehei and A. McEwan, "Differences in Power Spectral Densities and Phase Quantities Due to Processing of EEG Signals", *Sensors*, vol. 20, no. 21, p. 6285, 2020. Available: 10.3390/s20216285.
- [30] T. O. Zander, C. Kothe, S. Jatzev, and M. Gaertner, "Enhancing human-computer interaction with input from active and passive brain-computer interfaces," *Brain-Computer Interfaces*, pp. 181–199, 2010.
- [31] J. M. ten Have, "The development of the NLR ATC Research Simulator (narsim): Design philosophy and potential for ATM research," *Simulation Practice and Theory*, vol. 1, no. 1, pp. 31–39, 1993.
- [32] Emotiv, *EPOC+ User Manual*, 2021. Available: <https://emotiv.gitbook.io/epoc-user-manual/>
- [33] N.-H. Liu, C.-Y. Chiang, and H.-C. Chu, "Recognizing the degree of human attention using EEG signals from mobile sensors," *Sensors*, vol. 13, no. 8, pp. 10273–10286, 2013.
- [34] C.-J. Peng, Y.-C. Chen, C.-C. Chen, S.-J. Chen, B. Cagneau, and L. Chassagne, "An EEG-based attentiveness recognition system using Hilbert–Huang transform and support vector machine," *Journal of Medical and Biological Engineering*, vol. 40, no. 2, pp. 230–238, 2019.
- [35] H.H., Jasper, "International Federation of Societies for electroencephalography and clinical neurophysiology," *Electroencephalography and Clinical Neurophysiology*, vol. 10, no. 2, p. 367, 1958.
- [36] F. Faul, E. Erdfelder, A. Buchner and A. Lang, "Statistical power analyses using G*Power 3.1: Tests for correlation and regression analyses", *Behavior Research Methods*, vol. 41, no. 4, pp. 1149-1160, 2009. Available: 10.3758/brm.41.4.1149.
- [37] J. Medeiros, R. Couceiro, G. Duarte, J. Durães, J. Castelhana, C. Duarte, M. Castelo-Branco, H. Madeira, P. de Carvalho, and C. Teixeira, "Can EEG be adopted as a neuroscience reference for assessing software programmers' cognitive load?," *Sensors*, vol. 21, no. 7, p. 2338, 2021.
- [38] M. Teplán, "Fundamentals of EEG measurement," *Measurement Science Review*, vol. 2, no. 2, pp. 1–11, 2002.
- [39] D. F. Stegeman and M. J. Van Putten, "Recording of neural signals, neural activation, and signal processing," *Oxford Textbook of Clinical Neurology*, pp. 37–45, 2017.
- [40] P. J. Charles, R. J. Scwabassi and Mingui Sun, "Non-Gaussian modeling of EEG data," *Proceedings of the First Joint BMES/EMBS Conference. 1999 IEEE Engineering in Medicine and Biology 21st Annual Conference and the 1999 Annual Fall Meeting of the Biomedical Engineering Society (Cat. N)*, 1999, pp. 1023 vol.2-, doi: 10.1109/IEMBS.1999.804176.
- [41] Á. Costa, R. Salazar-Varas, A. Úbeda and J. Azorín, "Characterization of Artifacts Produced by Gel Displacement on Non-invasive Brain-Machine Interfaces during Ambulation", *Frontiers in Neuroscience*, vol. 10, 2016. Available: 10.3389/fnins.2016.00060.
- [42] R. Srinivasan, "Methods to improve spatial resolution of EEG," *International Journal of Bioelectromagnetism*, vol. 1, no. 1, pp. 102–111, 1988.
- [43] E. Düzel et al., "Task-related and item-related brain processes of memory retrieval", *Proceedings of the National Academy of Sciences*, vol. 96, no. 4, pp. 1794-1799, 1999. Available: 10.1073/pnas.96.4.1794.
- [44] H. Magen, T.-A. Emmanouil, S. A. McMains, S. Kastner, and A. Treisman, "Attentional demands predict short-term memory load response in posterior parietal cortex," *Neuropsychologia*, vol. 47, no. 8-9, pp. 1790–1798, 2009.
- [45] M. F. Rushworth, T. Paus, and P. K. Sipila, "Attention systems and the organization of the human parietal cortex," *The Journal of Neuroscience*, vol. 21, no. 14, pp. 5262–5271, 2001.
- [46] M. Behrmann, J. Geng and S. Shomstein, "Parietal cortex and attention", *Current Opinion in Neurobiology*, vol. 14, no. 2, pp. 212-217, 2004. Available: 10.1016/j.conb.2004.03.012.

- [47] A. C. Nobre, J. T. Coull, V. Walsh, and C. D. Frith, "Brain activations during visual search: Contributions of search efficiency versus feature binding," *NeuroImage*, vol. 18, no. 1, pp. 91–103, 2003.
- [48] H. Kojima and T. Suzuki, "Hemodynamic change in occipital lobe during visual search: Visual attention allocation measured with NIRS," *Neuropsychologia*, vol. 48, no. 1, pp. 349–352, 2010.
- [49] C. Colby and M. Goldberg, "SPACE and attention in parietal cortex", *Annual Review of Neuroscience*, vol. 22, no. 1, pp. 319-349, 1999. Available: 10.1146/annurev.neuro.22.1.319.
- [50] S. Kastner and L. G. Ungerleider, "Mechanisms of visual attention in the human cortex," *Annual Review of Neuroscience*, vol. 23, no. 1, pp. 315–341, 2000.
- [51] H. Stemmann and W. A. Freiwald, "Evidence for an attentional priority map in inferotemporal cortex," *Proceedings of the National Academy of Sciences*, vol. 116, no. 47, pp. 23797–23805, 2019.
- [52] R. H. Grabner, A. C. Neubauer and E. Stern, "Superior performance and neural efficiency: The impact of intelligence and expertise," *Brain Research Bulletin*, 69, 422–439, 2006.
- [53] R. H. Grabner, E. Stern and A. C. Neubauer, "When intelligence loses its impact: neural efficiency during reasoning in a familiar area," *International Journal of Psychophysiology*, 49, 89–98, 2003.
- [54] D. Nussbaumer, R. H. Grabner and E. Stern, "Neural efficiency in working memory tasks: The impact of task demand," *Intelligence*, 50, 196–208, 2015.